Macromol. Symp. **2004**, *212,* 375-380

Lattice Dynamics and Electron-Phonon Coupling in Pentacene Crystal Structures

Matteo Masino,[1] *Alberto Girlando,*[1] *Aldo Brillante,*[2] *Luca Farina,*[2]
Raffaele Guido Della Valle,[2] *Elisabetta Venuti*[2]

[1] Dip. Chimica GIAF, University of Parma, Viale delle Scienze 17, 43100 Parma, Italy
[2] Dip. Chimica Fisica e Inorganica, University of Bologna, Viale Risorgimento 4, 40136 Bologna, Italy

Summary: The crystal structures and lattice phonons of pentacene are computed by the quasi harmonic lattice dynamics (QHLD) method. From the eigenvectors of the low frequency phonons we calculate the *e-ph* coupling constants due to the modulation of the transfer integrals. The transfer integrals are computed by the Hückel method and by the INDO/S Hamiltonian for all the nearest neighbor pentacene pairs in the *ab* crystal plane.

Keywords: charge transport; conjugated materials; electron-phonon coupling; lattice dynamics; molecular crystals

Introduction

Pentacene is a well known organic semiconductor, recently object of renewed interest due to a report of very high charge carrier mobilities at low temperature in extremely pure single crystals.[1]

In the present paper we address the lattice phonon dynamics of pentacene, and their interactions with charge carriers, in order to provide a basis for the understanding of the above mentioned phenomena. Indeed, both the temperature dependence of the charge carriers mobilities and the onset of superconductivity have been ascribed to the electron-phonon coupling.[1]

Crystal structure and phonon dynamics

At the light of the five crystallographic analyses so far reported on a single crystal of pentacene,[2-5] the first problem we have to deal with is how many pentacene polymorphic structures exist and

DOI: 10.1002/masy.200450845

how these structures are related to the observed phenomena. On the basis of our recent theoretical[6] and experimental works[7] it is clear that pentacene shows at least two polymorphic structures. We have named the two polymorphs as phase **C** after the structure of Campbell et al.[2] and as phase **H** after the structure which results from the more recent crystallographic investigations.[3-5] The **H** phase is the phase on which all the most recent experiments have been done.[1]

To take into account the temperature effects and to describe vibrational properties, we employ the quasi-harmonic lattice dynamics (QHLD) method.[8,9] In QHLD the vibrational contribution to the Gibbs free energy, *G(p,T)*, is approximated with the Gibbs energy of the harmonic phonons:

$$G(p,T) = \Phi + pV + \sum_{\vec{q},j} \frac{\hbar\omega_{\vec{q},j}}{2} + k_B T \sum_{\vec{q},j} ln\left[1 - exp\left(-\frac{\hbar\omega_{\vec{q},j}}{k_B T}\right)\right]$$

where the intermolecular potential energy of the crystal, Φ, is represented by an atom-atom Buckingham model,[10] with Williams parameters set IV,[11] plus electrostatic interactions described by the *ab initio* atomic charges residing on the atoms. Given an initial lattice structure, one computes Φ and its second derivative with respect to the displacements of the molecular coordinates. The second derivatives form the dynamical matrix, which is numerically diagonalized to obtain the phonon frequencies and the corresponding eigenvectors. We allow for the mixing between lattice and intramolecular vibrations.[9] The equilibrium structure and phonon dynamics as a function of temperature are determined self-consistently by minimizing *G(p,T)* with respect to the unit cell axes, angles and molecular orientations.

Electronic structure

We have performed electronic structure calculation based on the tight-binding model on the two polymorphic crystal structures of pentacene to study how different packings affect the electronic properties. In the framework of the tight-binding model the band dispersion relations read:

$$\varepsilon_{\pm}(\vec{k}) = (t_{a1} + t_{a2})\cos\vec{k}\vec{a} \pm 4\left(t_{d1}\cos\vec{k}\,\frac{\vec{a}+\vec{b}}{2} + t_{d2}\cos\vec{k}\,\frac{\vec{a}-\vec{b}}{2}\right)$$

where the labelling of the *ab* crystal plane intermolecular transfer integral *t* is the same as in

Ref.[12]. The intermolecular transfer integrals have been estimated using two different quantum chemistry semiempirical methods: The extended Hückel method and the INDO/S Hamiltonian developed by Zerner and coworkers, with Mataga-Nishimoto repulsion potential.[13]

The results as a function of temperature and crystal structures are listed in Tab.1.

Table 1: Calculated VB and CB INDO/S bandwidths as a function of temperature and structure

Extended Hückel bandwidth				
Structure		*0 K*	*150 K*	*300 K*
H	valence band	203 meV	189 meV	169 meV
	conduction band	271 meV	255 meV	229 mev
C	valence band	159 meV	152 meV	135 meV
	conduction band	227 meV	217 meV	193 meV

INDO/S bandwidth				
Structure		*0 K*	*150 K*	*300 K*
H	valence band	632 meV	585 meV	536 meV
	conduction band	672 meV	624 meV	576 mev
C	valence band	548 meV	511 meV	470 meV
	conduction band	588 meV	548 meV	508 meV

The total valence and conduction band of the **H**-polymorph, which has been recognized as the one showing enhanced charge transport properties, are ~15-20% wider than in the **C**-polymorph. Moreover, as already pointed out by Brédas et al.,[12] the INDO/S method is able to reproduce large bandwidth values fully consistent with recent low temperature experimental estimates on the order of 500 meV.[14] These values are then considered more reliable than the simple extended Hückel estimates.

On the other hand, the observed sharp temperature dependence of the transport properties cannot be explained on the basis of bare band theory, since the calculated bandwidth reduction in going from room temperature to 0 K is on the order of 15-20%, to be compared with the experimental estimates of about 90%.[14] It is indeed commonly accepted that in acene crystals band transport is a typical situation at low temperature, but does not usually apply to higher temperature. As temperature increases, low energy vibrational modes start impeding the mobilities of the charge carriers. In this picture, therefore, the coupling between charge carriers and low frequency lattice phonons (*e-lph* coupling) is the key parameter governing charge transport.

E-lph coupling

Whereas extensive theoretical[15,16] and experimental[17] studies have been devoted to the characterization of the local contribution of the electron-phonon coupling, basically the variation of the on-site molecular energy with respect to the intramolecular vibrations, very little is known on the *e-lph* coupling. In molecular crystals, lattice phonons are expected to couple to charge carriers mainly modulating the amplitude of the intermolecular transfer integral. The corresponding linear *e-lph* coupling constants are defined as:

$$g(\vec{q},j)=\sqrt{\frac{\hbar}{2\omega_{\vec{q},j}}}\left(\frac{\partial t}{\partial Q_{\vec{q},j}}\right)_0$$

where $Q_{\vec{q},j}$ is the normal coordinate for the j-th phonon with wavevector $\vec{q}$. We have assumed that the optical lattice phonons as dispersionless, and have performed calculations for the $\vec{q}=0$ eigenvectors only. Within this approximation, symmetry arguments show that only the totally symmetric phonons can be coupled to charge carriers. To evaluate the *e-lph* coupling constants we have calculated each intermolecular transfer integral for the equilibrium geometry, as well as for geometries displaced along the QHLD eigenvectors. The various $g(\vec{q},j)$ are then obtained by numerical differentiation. The *e-lph* coupling constants for the four largest transfer integrals calculated using the INDO/S Hamiltonian are reported in Tab.2.

We can compare the calculated *e-lph* coupling constants with tunneling experiments.[18] Indeed, the conductance derivative spectrum d^2I/dV^2, shown in Fig.1 is proportional to the phonon density of states weighted by an effective electron-phonon coupling function.

Table 2 shows that, although some differences exist, the most strongly coupled modes for both valence and conduction band occur around 25, 19, 12, 8 and 3 meV. The first four modes find correspondence in the experimental tunneling spectrum of Fig.1, where one sees a strong doublet centered at 25 meV, a broad peak at 8 meV and two minor features around 16 and 13 meV. Moreover, our calculations also predict that the lowest energy phonon at 3.4 meV, difficult to access in the tunneling experiment,[18] should be strongly coupled to charge carriers. We associate this phonon mode to the most intense band observed at 4.6 meV in the Raman spectra of **H** pentacene.[7]

Table 2: Low-energy A_g phonons and *e-lph* coupling constants of **H** pentacene calculated at 0 K (me V)

	Valence band				*Conduction band*			
ω	g_{a1}	g_{a2}	g_{d1}	g_{d2}	g_{a1}	g_{a2}	g_{d1}	g_{d2}
38.4	0.0	0.1	-1.0	0.8	0.0	0.0	1.2	1.1
38.0	0.0	-0.2	-0.3	-0.1	0.0	0.0	0.0	0.0
32.4	-0.1	0.3	-2.4	-1.6	0.0	0.0	-1.4	-1.0
32.1	0.7	0.0	2.7	2.0	-0.3	0.0	1.6	1.5
29.9	0.1	1.4	-1.0	-1.5	0.0	-0.5	0.7	1.3
29.5	1.8	-0.2	1.8	0.3	-0.7	0.0	-0.8	0.0
25.5	0.4	0.0	-1.6	-1.6	-0.9	0.9	1.2	1.8
25.2	-0.4	0.0	3.1	4.5	0.8	0.7	1.2	2.8
20.1	-0.1	1.2	-0.9	-1.7	0.4	-1.4	-0.1	-0.5
19.3	-0.4	0.2	-0.8	-2.8	-1.6	-0.4	-0.7	-3.2
18.4	0.2	0.0	-2.1	-5.0	0.0	0.0	0.0	0.0
16.4	-0.5	-1.0	1.8	0.8	0.5	1.0	-0.4	-0.1
11.9	-0.6	0.0	3.2	1.1	1.0	0.3	-4.3	-2.5
8.7	4.0	-3.0	0.9	-1.4	-2.2	1.7	2.0	1.6
7.6	-1.6	-3.2	-3.6	1.3	1.4	1.2	0.0	2.3
3.4	3.6	4.5	1.5	-1.4	-1.1	-2.5	-3.2	-0.4

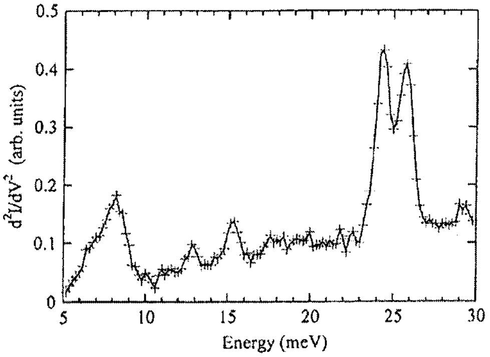

Fig.1: Conductance derivative spectrum of **H** pentacene at 1.4 K. From Ref.[18]

Conclusions

We have calculated the crystal structures, phonon dynamics and electronic structure of both pentacene polymorphs as a function of temperature. Band structure calculations based on tight-binding model can be exploited to reproduce estimated experimental bandwidth of high purity sample at low temperature. The electron-phonon coupling has to be invoked in order to account for the sharp temperature dependence. We, therefore, have fully characterized the interaction between holes/electrons and the low frequency optical phonons, paving the way to understand charge transport properties in pentacene.

[1] J. H. Schön et al., *Phys. Stat. Sol. B* **2001**, 226, 257; *Science* **2000**, 288, 2338; *Nature* **2000**, 406, 702.
[2] R. B. Campbell, J. M. Robertson, J. Trotter, *Acta Cryst.*, **1962**, 15, 289.
[3] D. Holmes, S. Kumaraswamy, A. J. Matzger and K. P. Vollhardt; *Chem. Eur. J.*, **1999**, 5, 3399.
[4] T. Siegrist et al., *Angew. Chem. Int. Ed.*, **2001**, 40, 1732.
[5] C. C. Mattheus, A. B. Dros, J. Baas, A. Meetsma, J. de Boer and T. T. M. Palstra, *Acta Cryst. C*, **2001**, 57, 939.
[6] E. Venuti, R. G. Della Valle, A. Brillante, M. Masino and A. Girlando, *JACS*, **2001**, 124, 2128.
[7] A. Brillante, R. G. Della Valle, L. Farina, A. Girlando, M. Masino, E. Venuti, *Chem. Phys. Lett.*, **2002**, 357, 32.
[8] R. G. Della Valle, E. Venuti and A. Brillante, *Chem. Phys.*, **1996**, 202, 231.
[9] A. Girlando, M. Masino, G. Visentini, R. G. Della Valle, A. Brillante, E. Venuti, *Phys. Rev. B*, **2000**, 62, 14476.
[10] A. J. Pertsin and A. I. Kitaigorodsky, *"The atom-atom potential method"* Springer-Verlag, Berlin, 1987.
[11] D. E. Williams, *J. Chem. Phys.*, **1967**, 47, 4680.
[12] J. Cornil, J. Ph. Calbert, J. L. Brédas, *JACS*, **2001**, 123, 1250.
[13] J. Ridely and M. C. Zerner, *Theor. Chim. Acta*, **1973**, 32, 111.
[14] J. H. Schön, C. Kloc and B. Batllogg, *Phys. Rev. Lett.*, **2001**, 86, 3843.
[15] A. Devos, M. Lannoo, *Phys. Rev. B*, **1998**, 58, 8236.
[16] T. Kato, T. Yamabe, *J. Chem. Phys.*, **2001**, 115, 8592.
[17] N. Gruhn, D.da Silva Filho, T. Bill, M. Malagoli, V. Coropceanu, A. Kahn, J.L. Brédas, *JACS*, **2002**, 124, 7918.
[18] M. Lee, J. H. Schön, Ch. Kloc and B. Batlogg, *Phys. Rev. Lett.*, **2001**, 86, 862.